

Derivative-assisted evaluation of well yields in a heterogeneous aquifer

Kevin P. Parks and Laurence R. Bentley

Abstract: The evaluation of well yields with conventional time-drawdown methods is based on the assumption of infinite-acting radial flow (IARF) of groundwater to a well. However, long-term well yields are controlled by heterogeneities and, as suggested here, by the presence of linear features and aquitard leakage, and the subsequent departures from IARF. Accurate prediction of long-term well yields therefore requires an evaluation of aquifer heterogeneities. Derivative techniques combined with aquifer geology and conventional methods aid in the evaluation of long-term well yields in heterogeneous aquifers. Our case study involves the estimation of long-term well yields from relatively short-term aquifer tests in an aquifer near Calgary, Alberta. The wells are completed in a gravel-floored channel incised into bedrock. On the regional scale, the floor gravels appear to form a continuous and homogeneous aquifer. Aquifer-test responses indicate internal heterogeneity at a scale below the resolution attainable with the available well control. Reliable estimates of aquifer parameters are obtained by applying a derivative technique to the analysis of time-drawdown data. Derivative analysis allows us to isolate test segments for which the assumption of IARF is valid. Characteristic time-drawdown and derivative curves are then integrated with geology to identify the nature of heterogeneities and assess their impact on long-term aquifer response to pumping.

Key words: aquifer test, derivative, heterogeneity, well yield, buried valley aquifer.

Résumé : L'évaluation des débits d'un puits au moyen des méthodes conventionnelles de rabattement en fonction du temps est basée sur l'hypothèse d'écoulement radial à l'infini (IARF) de l'eau souterraine vers un puits. Cependant, les débits à long terme sont contrôlés par les hétérogénéités, et tel que suggéré ici, par la présence de caractéristiques linéaires et de fuites dans l'aquitard, et par les déviations subséquentes dans l'IARF. La prédiction précise des débits à long terme d'un puits dans des aquifères hétérogènes requièrent donc une évaluation des hétérogénéités de l'aquifère. Des techniques de dérivation combinées avec la géologie de l'aquifère et les méthodes conventionnelles aident à évaluer les débits à long terme d'un puits dans des aquifères hétérogènes. Notre étude de cas implique l'estimation à long terme des débits d'un puits en partant d'essais d'aquifère à relativement court terme dans un aquifère près de Calgary, Alberta. Les puits se sont terminés dans un lit de gravier d'un canal incrusté dans le lit rocheux. À l'échelle régionale, les graviers du lit semblent former un aquifère continu et homogène. Les essais de réponse de l'aquifère indiquent une hétérogénéité interne à une échelle inférieure à la résolution atteignable avec le puits de contrôle disponible. Des estimés fiables des paramètres de l'aquifère sont obtenus en appliquant la technique de dérivation à l'analyse des données de rabattement en fonction du temps. L'analyse par dérivation nous permet d'isoler des segments d'essais pour lesquels l'hypothèse d'IARF est valide. Les courbes caractéristiques de rabattement en fonction du temps et de dérivation sont alors intégrées à la géologie pour identifier la nature des hétérogénéités et évaluer leur impact sur la réponse au pompage de l'aquifère à long terme.

Mots clés : essai d'aquifère, dérivation, hétérogénéité, débit de puits, aquifère de vallée enfouie.

[Traduit par la rédaction]

Introduction

Drawdown-derivative analysis is a straightforward analytical tool for aquifer-test interpretation. The drawdown derivative is the first derivative of drawdown in an aquifer during pumping taken with respect to the natural logarithm of time. When plotted against time, the derivative profile can identify which time-drawdown data represent infinite-acting

radial flow (IARF) to a well and to which the Theis or Cooper-Jacob solutions for estimating aquifer transmissivity (T) and storativity (S) are applicable. Derivative analysis as an aid to aquifer-test interpretation was introduced to the groundwater literature by Karasaki et al. (1988) and Spane and Wurster (1993). Its origins go back about a decade prior in the petroleum engineering literature, specifically the paper by Bourdet et al. (1983).

Despite its utility, derivative analysis remains both under-used and under-reported in the hydrogeology literature. The under-reporting probably reflects the bias in the technical literature against commonplace case studies in groundwater-supply evaluation, a bias that impedes

Received June 14, 1995. Accepted February 21, 1996.

K.P. Parks and L.R. Bentley, Department of Geology and Geophysics, University of Calgary, Calgary, AB T2N 1N4, Canada.

widespread and rapid dissemination of “new” approaches to help solve an “old” problem, namely the estimation of aquifer T and S . The under-use of derivatives by practicing hydrogeologists may be due, in part, to the subtleties involved in effectively coding the derivative calculation and smoothing algorithms. Widespread dissemination of robust public-domain codes like DERIV by Spane and Wurstner (1993) will help overcome this obstacle. The under-use may also be due to a lack of published case studies demonstrating the strengths and weaknesses of derivative techniques as applied to conventional aquifer-test analysis.

The purpose of our paper is to help correct this situation. We demonstrate the use of drawdown-derivative analysis in groundwater evaluation of a heterogeneous aquifer that exhibits various familiar, yet problematic, hydraulic behaviours during aquifer tests. We show that the drawdown-derivative analysis improves our estimation of aquifer hydraulic properties and prediction of probable long-term well yields. Shortfalls of the technique are also shown.

Derivative analysis

During an aquifer test, the hydraulic head in the aquifer declines as the time of pumping increases. Analysis of hydraulic head decline, or drawdown, behaviour allows for the estimation of aquifer hydraulic properties. However, log-log type curve analyses of time-drawdown data based on the Theis solution suffer from problems of non-uniqueness. Semilog plots based on the Cooper-Jacob solution are better in this respect, but it can be hard to identify which part of a multisegmented semilog time-drawdown curve satisfies the inherent assumption of infinite acting radial flow (IARF) to the well.

The drawdown derivative is defined as the first derivative of drawdown with respect to the natural logarithm of time. It is very sensitive to variations in flow due to well-bore storage effects and aquifer non-idealities. Its sensitivity reduces the non-uniqueness problem when applied to type-curve methods. Drawdown-derivative curves have characteristic profiles that permit identification of flow-regime types in an aquifer. The profiles can also be used to identify which segments of semilog time-drawdown curves represent well-bore storage effects and which satisfy the assumption of IARF. Spane and Wurstner (1993) review the genealogy of drawdown-derivative analysis and its application to constant-rate discharge and slug tests in hydrogeology. Details of derivative analysis are also reported in Wong et al. (1986), Karasaki et al. (1988), Ehlig-Economides (1988), Ostrowski and Kloska (1989), and Bourdet et al. (1989).

There are difficulties inherent in the application of derivative techniques to aquifer-test analysis. Calculation of the derivative from test data is a noise-producing process. Irregular fluctuations in drawdown during an aquifer test, say from pump surge, can create noise in the derivative plot that confounds the analysis. Sparse data sets are especially prone to noisy derivative plots; regular and dense measurement of drawdown using an automatic data logger produces the best results. Smoothing algorithms like those employed in the DERIV program seek to reduce the noise

inherent in the differentiation step by filtering. Successful application of the smoothing algorithm is not a trivial step in derivative analysis, as discussed by Spane and Wurstner (1993).

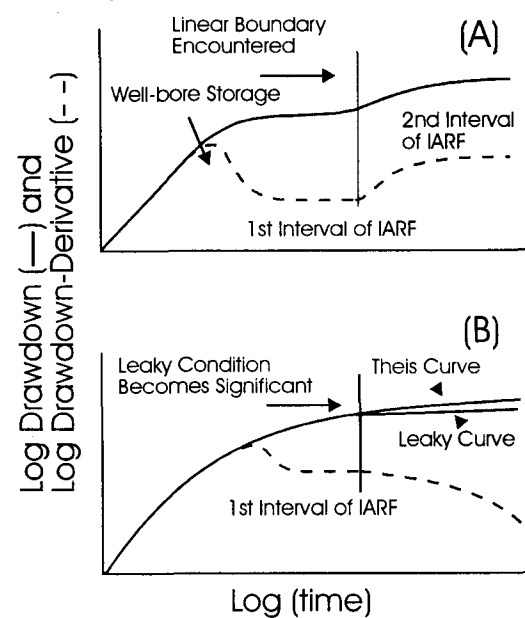
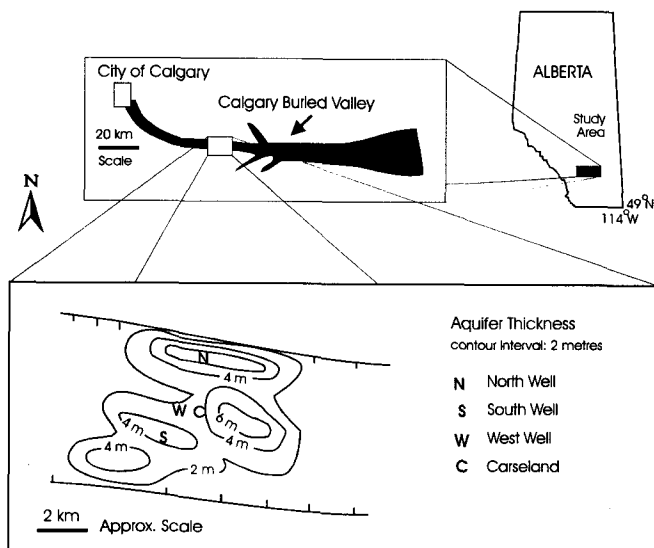


Figure 1 shows characteristic log-log time-drawdown and derivative behaviour for three simple systems commonly encountered in aquifer-test analysis. The early-time drawdown curve in Fig. 1A represents an ideal confined aquifer with well-bore storage. The drawdown and derivative at early test times both increase with a unit slope on the log-log plot. This behaviour is characteristic of pure well-bore storage effects. Thereafter, the time-drawdown curve develops the characteristic curvature of the Theis well function. The derivative curve in contrast, passes over a hump during transition from pure well-bore storage effects and then flattens out to a constant value. The horizontal line segment marks the first interval of IARF, wherein a straight line will be observed on a semilog Cooper-Jacob plot, i.e., $\delta s/\delta(\ln t) = Q/4\pi T$, where s is drawdown, t is time, and Q is a discharge rate.

Early-time aquifer-test data can be used in conjunction with the derivative to identify segments of time in which IARF is present prior to the onset of a constant slope on a Cooper-Jacob plot. The analyst has to be confident, however, that the early-time data are not contaminated by bore-hole or casing storage effects in order to proceed with type-curve analysis. Otherwise the analyst is forced to account for these effects explicitly. The practice of using only the constant, horizontal segments of the derivative

only the constant, horizontal segments of the derivative

Fig. 2. Location of study area in Alberta, Canada. The Calgary Buried Valley System is a valley incised into bedrock now infilled mostly with glacial till. Saturated alluvial deposits on the valley floor comprise a major regional aquifer. On a local scale, alluvial heterogeneities form lenticular patterns of aquifer thickness but no other heterogeneities are visible. This study concerns hydraulic response in this aquifer at three municipal wells near the Hamlet of Carseland, Alberta, southeast of the city of Calgary.



profile to identify an interval of IARF to the well is a pragmatic solution to the difficulty of assessing the reliability of early-time aquifer-test data. As well, early test data are usually most sparse with respect to the logarithm of time and most likely affected by mechanical adjustments in the test apparatus at the beginning of the test. The derivative will therefore usually be the most noisy for this interval.

The sensitivity of the derivative to small changes in drawdown is also its strength in helping the analyst interpret heterogeneous aquifer-system responses to pumping stress. For example, time-drawdown behaviour in the presence of a linear boundary is also shown in Fig. 1A. A boundary causes the late-time drawdown curve to rise above the Theis well function and the derivative curve to rise to another horizontal line where $\delta s/\delta(\ln t) = 2Q/4\pi T$, corresponding to the doubling of the slope on a semilog Cooper-Jacob plot after the cone of depression encounters the boundary.

Derivative behaviour in the presence of leakage is demonstrated in Fig. 1B. Leakage from confining beds causes the log-log time-drawdown curve to rise at a rate less than the Theis curve. On a semilog Cooper-Jacob plot, leakage is detected by a reduction in the slope of the time-drawdown curve. Note in Fig. 1B that in a leakage case, the affected segment of the drawdown-derivative continuously declines in value with time. If the leakage became sufficient to match well discharge, the drawdown will become constant and the value of the derivative would fall to zero (or become asymptotic to a vertical line on a log-log plot).

Characteristic derivative behaviour has likewise been described for wells encountering unconfined conditions, recharge boundaries (Spang and Wurster 1993), vertical faults, hydraulic fractures, and dual-porosity (fracture-block) systems (Bourdet et al. 1989).

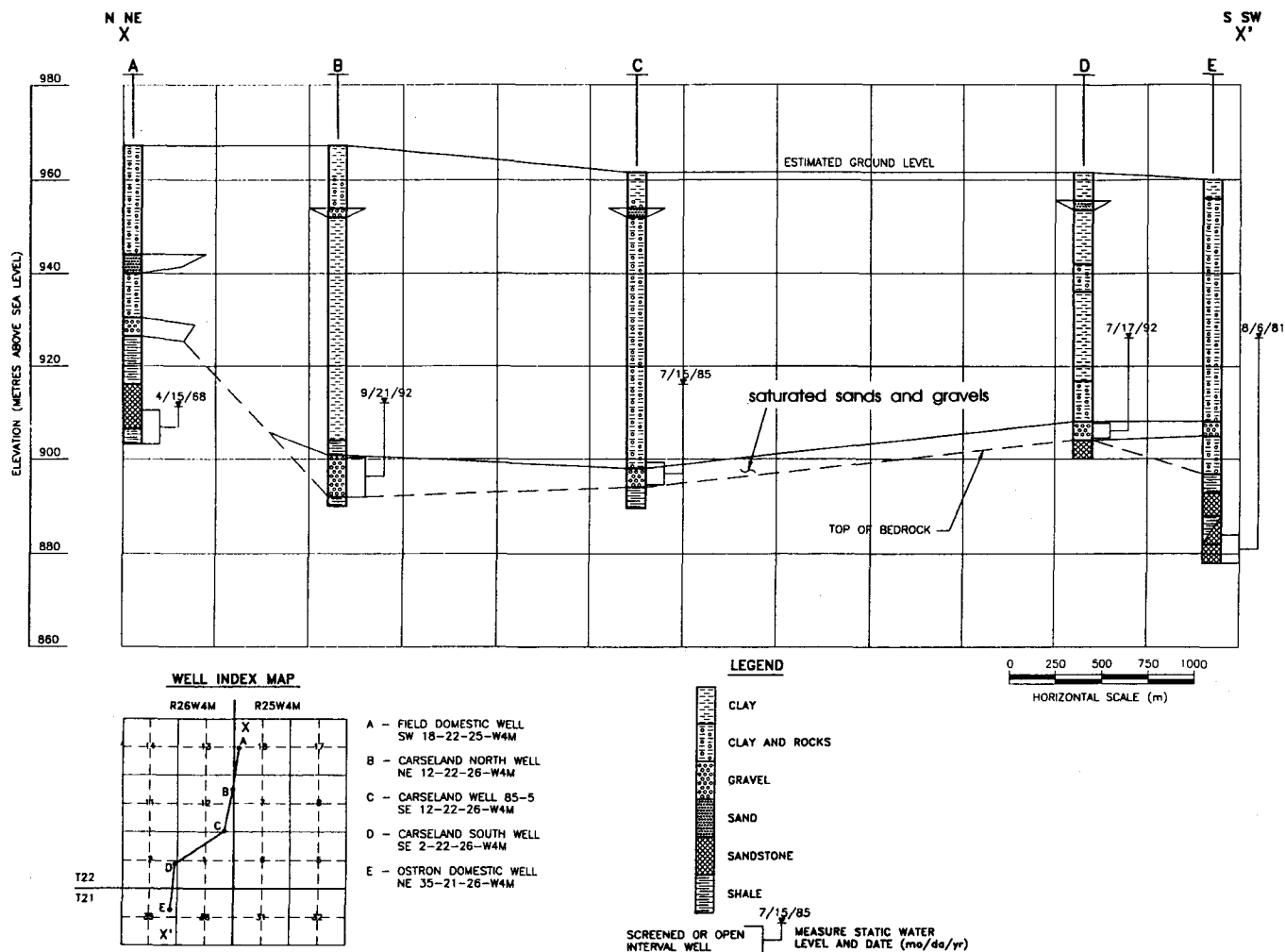
Case study in the Calgary Valley aquifer, Alberta

Gravel-floored buried bedrock valleys form major aquifer systems in the formerly glaciated plains region of western Canada (Lennox et al. 1988). In Alberta and Saskatchewan, these aquifers often provide the only assured supply of reasonable quality water for agriculture and domestic consumption. When mapped at a scale defined by available well density, usually one well per square-mile section (1 square mile = 2.589988 km²), the gravel aquifers at the base of these valleys appear as continuous blankets.

Such simple aquifer geometry masks significant internal heterogeneity that will control long-term yields to water wells. Alluvial-aquifer systems are composed of architectural elements that are unique assemblages of lithofacies of characteristic geometry, existing within a hierarchy of spatial scales and possessing differing bulk hydraulic properties (Anderson 1990). In addition, hydraulic barriers are formed both transverse and longitudinal to the course of buried valley aquifers by pre- and postdepositional erosional processes, such as the formation of clay-filled cross-cutting glacial meltwater channels (Shaver and Puse 1992). Because the characteristic lengths of these elements are tens to hundreds of metres, they will be invisible on geological maps developed from wells spaced thousands of metres apart. Nevertheless, these elements will affect the radial flow of water to wells if they manifest themselves on the scale of the cone of depression (Desbarats 1994). A challenge in the development of buried valley aquifers is to account for the hydraulic effects of alluvial heterogeneities in predictions of long-term well yields.

The Calgary Valley extends from the city of Calgary eastward to the Alberta-Saskatchewan border (Fig. 2). At its western limit, the modern Bow River and Elbow River have reexposed the floor of the paleo-valley. At its eastern limit, the valley broadens and loses its defining valley shape (Geiger 1968). The Calgary Valley is asymmetrical in cross section, with a broad, shallow-dipping north flank and a sharp, steep-dipping south flank (Carlson et al. 1969). Locally, the valley flanks have gravel-topped terraces. The valley of the modern Bow River carves downwards into the Calgary Valley at several places along its course, exposing and reworking its floor gravels as modern alluvium. For most of its course, however, the Calgary Valley is filled with glacial till up to grade with the surrounding prairie and has no distinguishing surface expression. The valley-floor alluvial deposits are usually saturated and comprise a significant regional aquifer. Terrace gravels may also be saturated and are used as a source of groundwater in low-yield domestic wells. Long-term yields are in the range of 165–655 m³/d (25–100 igpm (imperial gallons per minute)), higher where they have been reworked and incorporated into modern alluvium by the Bow River where it downcuts to the base of the Calgary Valley (Ozora and Lytviak 1974).

Fig. 3. North-south cross section through the Calgary Buried Valley Aquifer. The aquifer appears as a thin sheet of sand and gravel at the valley base. No significant heterogeneities or discontinuities are mappable at this scale.



Our study area is at the hamlet of Carseland, Alberta, 40 km east of the city of Calgary. All of Carseland's municipal wells are completed in the Calgary Valley aquifer. An isopach map of the valley-floor alluvium in the Carseland area interpreted from water-well drillers' reports is in Fig. 2. The alluvium ranges in thickness from 1 m to over 8 m. At this scale, the aquifer heterogeneity is expressed as a pattern of thick lenses elongate parallel to the valley walls. No other heterogeneity is evident. A north-south cross section through the Calgary Valley is shown in Fig. 3. The aquifer appears as a thin sheet of sand and gravel at the valley base. Again, no significant heterogeneities or discontinuities appear at this scale.

Application of derivatives to aquifer-test analysis

This section describes the integration of drawdown-derivative analysis with the conventional interpretation of time-drawdown data from three aquifer tests in the Carseland well field. The wells are referred to as the south well, the west well, and the north well. In this study, we use

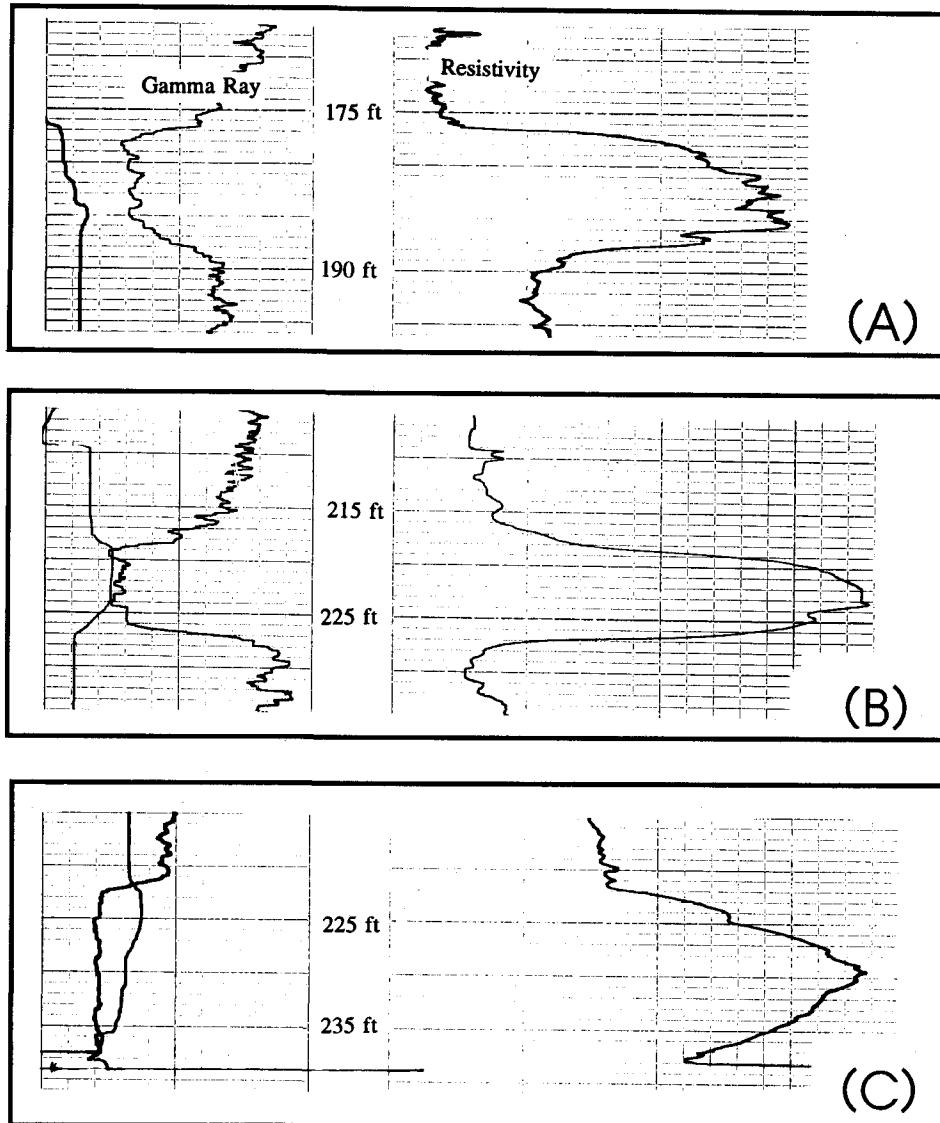
the program DERIV (Spang and Wurster 1993) to calculate drawdown derivatives from well test data.

South well

The south well is located 2 km southwest of Carseland at Dominion Land Survey (DLS) coordinates SE-2-22-26 W4M (see Fig. 2). The top of the sand and gravel deposits are 53.5 m (175 feet) below ground. The aquifer is about 3.5 m thick. Traces of resistivity and gamma-ray logs through the aquifer zone are shown in Fig. 4A. The static water level was 23 m above the base of the aquifer on the date of the test. During the test, the south well was pumped for 24 h at a constant rate of 196 m³/d (30 igpm). Water levels were monitored in the pumped well and in an observation well located 60 m south.

The Cooper-Jacob semilog time-drawdown plot for the south pumping well is shown in Fig. 5A. The corresponding derivative plot is shown in Fig. 5B. The Theis log-log and the Cooper-Jacob semilog time-drawdown plots for the south observation well data are shown in Figs. 6A and 6B, respectively. The drawdown derivative for the south observation well data is in Fig. 6C.

Fig. 4. Gamma-ray (left) and resistivity (right) traces in the Calgary aquifer alluvium at (A) the Carseland south well, (B) the Carseland west well, and (C) the Carseland north well. Leftward deflections of the gamma ray trace indicate sediments with a low abundance of radioactive grains, usually assumed to be clays. Rightward deflections of the resistivity trace indicate increased electrical resistance and lower clay abundance. Vertical scale is in feet. Leftmost trace is the caliper.



Although somewhat noisy, the south pumping well data on the Cooper-Jacob plot fall on two semilog straight-line segments. For this and all subsequent analyses, we use a criteria of $u < 0.1$, where $u = r^2 S / 4 T t$, as the practical cut-off for applicability of the Cooper-Jacob approximation (Kruseman and de Ridder 1990, p. 67). The slope of the first semilog straight line is 0.64 m per log cycle. The slope of the second semilog straight line segment is 1.12 m per log cycle. The apparent near-doubling of the semilog slope from the early segment to the late segment suggests a linear-type boundary in the vicinity of the pumping well. We return to the issue of a boundary later in this discussion.

The drawdown derivative is shown in Fig. 5B with two different smoothing parameters. The lighter, erratic solid line

is the derivative calculated with DERIV using an L-spacing of 0.1. This means that the derivative was calculated using a least-squares regression over a window of data centred on each point that had a half-width of 0.1 in units of $\log(\text{time})$. The heavier and smoother solid line on the derivative plot is the drawdown derivative for the same south pumping well data, only using a broader L-spacing of 0.4.

The sensitivity of the drawdown derivative to the choice of smoothing parameter is evident. The less-smoothed derivative profile is noisy but may show a stable range of derivative values during the interval from about $t = 10$ min to about $t = 100$ min. Thereafter the derivative follows an increasing trend to the end of the test. The more smoothed derivative profile starts its rise after about $t = 28$ min.

This early and continuous rise contradicts the two straight-line segments apparent on the corresponding Cooper-Jacob plot. We interpret the continuous rise in the derivative as an artifact of the loss of temporal resolution as the smoothing filter is broadened. No clearly definable second plateau of constant derivative value that would correspond to the second semilog straight line on Fig. 5A is observed in Fig. 5B for either choice of *L*-spacing.

Water levels in the observation well responded to pumping after about 5 min (Figs. 6A, 6B). On the Theis log-log plot, the best fit is achieved when data from the time interval from about *t* = 30 min to *t* = 300 min are fitted to the Theis curve. The early data appear contaminated by well-bore effects. The late data rise above the Theis curve and thus may be affected by a linear boundary in the vicinity of the pumping well. The type-curve match gives an estimate of *T* of 51 m²/d and *S* of 9.3 × 10⁻⁵.

On the Cooper-Jacob plot in Fig. 6B, the drawdown increases on a semilog linear trend from about *t* = 15 min until a break in slope evident at about *t* = 150 min. A second semilog linear trend is established after *t* = 500 min. The slope of the first semilog segment is about 0.67 m/log cycle. The slope of the second semilog segment is about 1.18 m/log cycle.

The log-log plot of drawdown derivative versus time for the south observation well data is shown in Fig. 6C. The initial data form a characteristic "hump" usually ascribed to well-bore storage effects in a pumped well. The hump suggests contamination of the early-time data from well-bore storage effects. Indeed, inspection of the Theis curve match shown in Fig. 6A supports this interpretation. The derivative calculated with an *L*-spacing of 0.4 stabilizes within a constant range from *t* = 40 min to about *t* = 110 min. The value of the derivative rises thereafter. The derivative calculated with an *L*-spacing of 0.1 shows a shorter stable interval during early test time, rising thereafter on a trend until it stabilizes within a constant range of values between after 600 min of pumping.

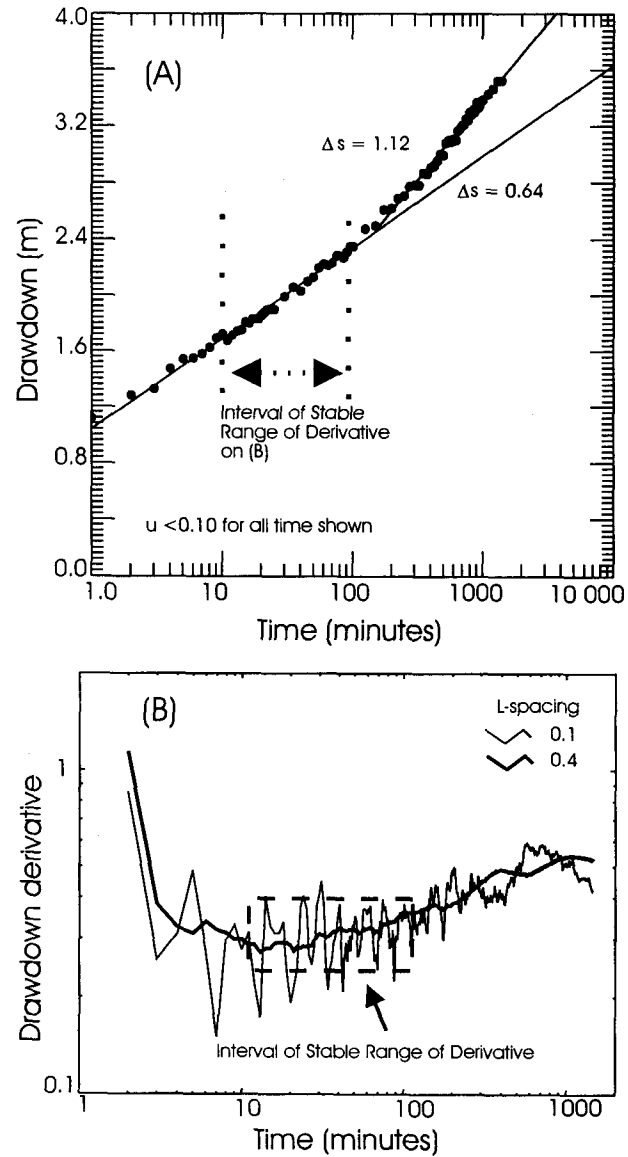
Inspection of the stable ranges of the derivative profile on Fig. 6C helps us to choose the best segments for Cooper-Jacob analysis. The first time interval, from *t* = 30 min to about *t* = 120 min may be most representative of IARF conditions near the pumping well. The transmissivity estimated by the Cooper-Jacob method from the slope of the corresponding time-drawdown segment is 54 m²/d. The same data provide an estimate of storativity of about 1 × 10⁻⁴. The value of *T* from the pumping well data for the first semilog straight line corresponding to the only observed interval with a stable derivative (*t* = 10–28 min) is about the same, 56 m²/d. These values compare favourably to the values of *T* and *S* obtained from the Theis curve analysis.

Analysis of the linear boundary

All of the time-drawdown and drawdown-derivative plots in Figs. 5 and 6 suggest a linear boundary in the vicinity of the south pumping well. The derivative is supposedly more sensitive to variations in aquifer response to pumping stresses and therefore may be used to improve our analysis of the distance to this supposed boundary.

The distance to a linear boundary from a pumping well can be approximated with the Cooper-Jacob equation for

Fig. 5. Cooper-Jacob semilog plot of time-drawdown data (A) and log-log plot of drawdown derivative versus time (B) for data from the Carseland south pumping well. Two semilog straight-line segments are evident on A. The first segment corresponds to an interval of stable range of derivative values noted on B (*L*-spacing = 0.1). No interval of stable range of derivative is noted for the late-time data for either *L*-spacing.



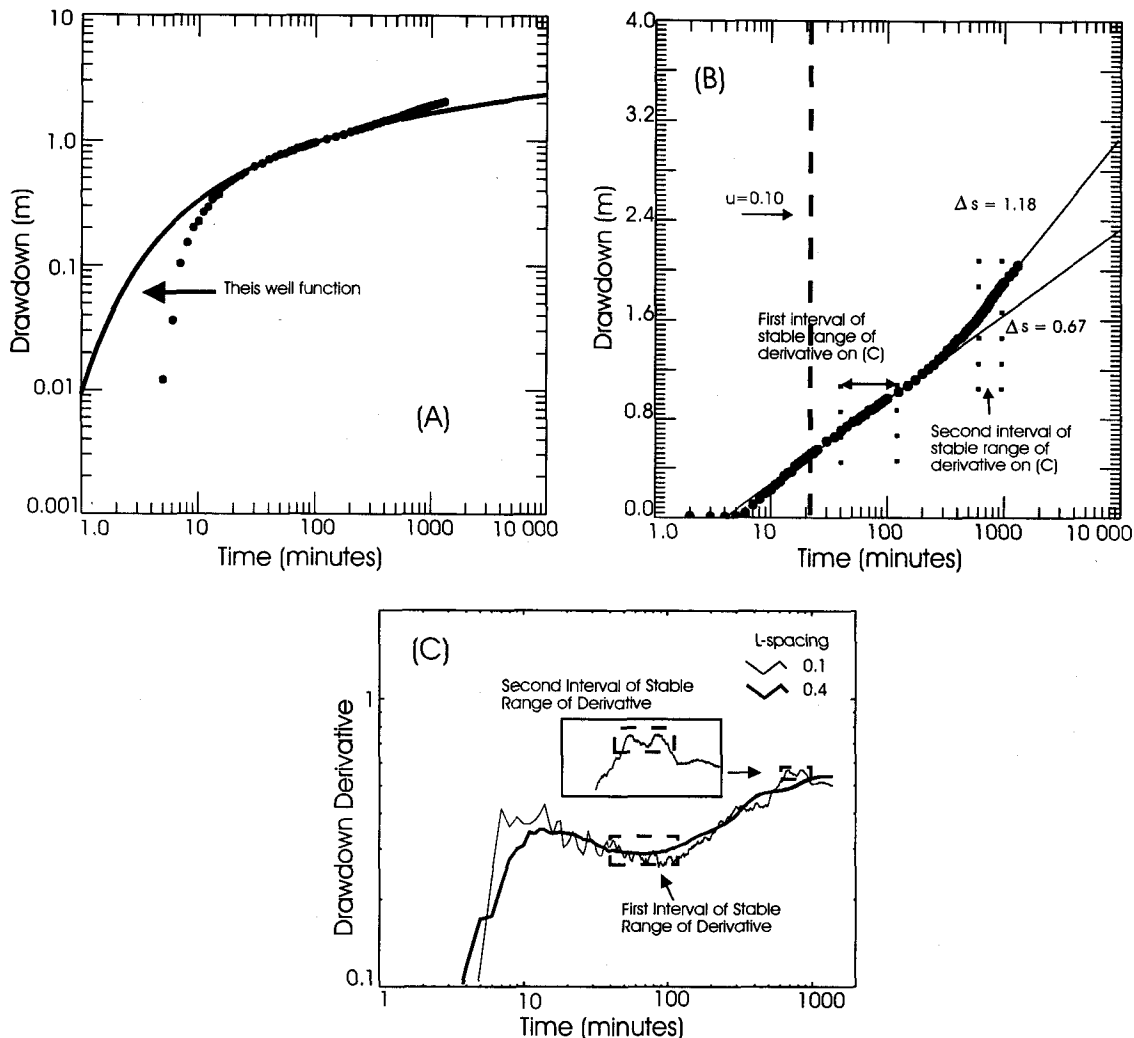
drawdown and image well theory (deMarsily 1986; p. 170). The Cooper-Jacob approximation for drawdown is

$$[1] \quad s = \frac{2.30Q}{4\pi T} \log_{10} \left(2.25 \frac{Tt}{r^2 S} \right)$$

where *s* is drawdown [L] at some radial distance *r* [L] from a well discharging at a rate *Q* [L³/T] for a time *t* [T] in a confined, homogeneous, horizontal, infinite aquifer with a constant transmissivity *T* [L²/T] and storativity *S* [-].

Setting the term inside the decalog operator to 1 (so drawdown *s* is zero) and solving for *r* using *t*_{end}, the end of

Fig. 6. Theis curve match (A), Cooper-Jacob semilog plot of time-drawdown data (B), and log-log plot of drawdown derivative versus time (C) for the Carseland south observation well. Early-time data on Theis plot show contamination by well-bore effects, late-time data suggest presence of a boundary. Two semilog straight-line segments are evident in B. The two semilog straight-line segments correspond to interpreted intervals of stable range of derivative values noted in C.



IARF on a Cooper-Jacob plot, provides an estimate of r_{image} , the distance from the pumping well to an image well on the other side of the boundary. The boundary itself will be located somewhere on a circle of radius $0.5r_{\text{image}}$ from the pumping well.

There are two approaches to selection of t_{end} in the presence of a linear boundary. One approach is to forward extrapolate the first semilog straight line in time until it intersects the backward extrapolation of the second semilog straight line drawn through late-time data. The time correspondent to the intersection of the two lines is taken as t_{end} . A second approach is to use the first departure from the semilog straight line as t_{end} . We favour the second approach as being more physically meaningful when considered in the context of a superposition model of the effects of linear boundaries (e.g., Kucuk and Kabir 1988).

If the second approach is used, then the drawdown derivative is of utility in determining t_{end} because it is more sensitive to the change in flow conditions to the

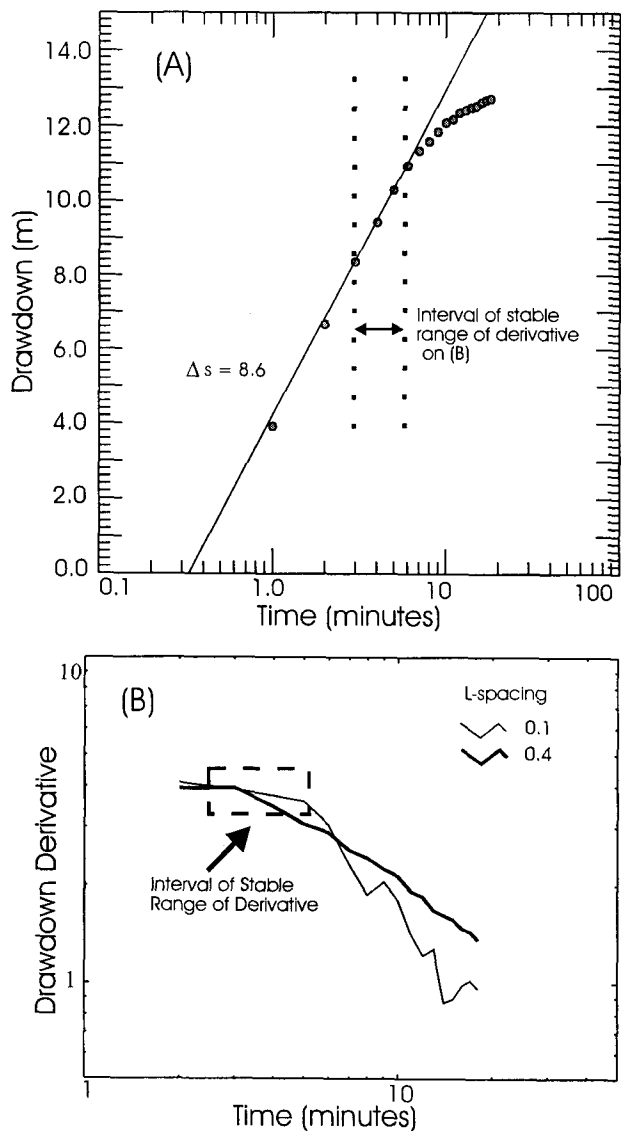
pumping well caused by the boundary. As discussed above, we interpret a change from a stable to a rising derivative, i.e., t_{end} , after about 100 min of pumping in Fig. 5B. Using the hydraulic parameters of $T = 56 \text{ m}^2/\text{d}$ and $S = 9.5 \times 10^{-5}$, the boundary should be found somewhere on a circle of a radius of about 150 m from the pumping well. A similar analysis can be made with the observation well data to better identify the actual location of the boundary.

It is of interest to note that no linear boundaries within that radius can be discerned from the aquifer geology as shown in Fig. 2. This observation might lead the hydrogeologist delineating groundwater resources to suspect the linear boundary is a cross-cutting shale-filled channel or a prominent bedrock ridge that cannot be mapped from available well data.

West well

The west well is located 1 km west of Carseland at DLS coordinates SE-11-22-26 W4M (see Fig. 2). The top of

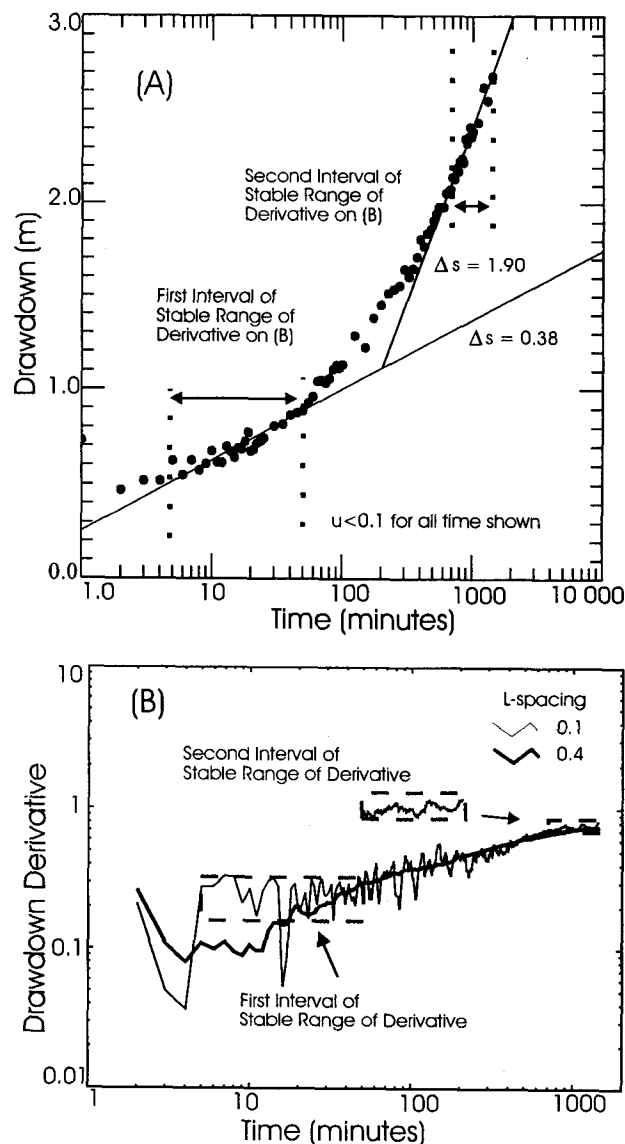
Fig. 7. Cooper-Jacob semilog plot of time–drawdown data (A) and log–log plot of drawdown derivative versus time (B) for the Carseland west well. Leakage or recharge is apparent in both plots after about 5 min of pumping.



the sand and gravel deposits are 66 m (216 feet) below ground. The aquifer is about 2.7 m thick. The static water level was 25 m above the base of the aquifer on the date of the test. Traces of resistivity and gamma-ray logs through the aquifer zone are shown in Fig. 4B. Due to mechanical problems during the test, the west well was pumped for only 30 min at a constant rate of 50 m³/d (11 igpm). Water levels were monitored in the pumped well.

Figure 7A is a Cooper-Jacob semilog plot of the time–drawdown data. Two intervals of approximately constant semilog slope are evident. Because the test was so short it is unclear from this plot alone whether the first semilog straight line represents borehole effects and the second and shorter semilog straight line represents true IARF response in the aquifer, or if the first segment represents true IARF response and the second shorter segment represents a leakage condition.

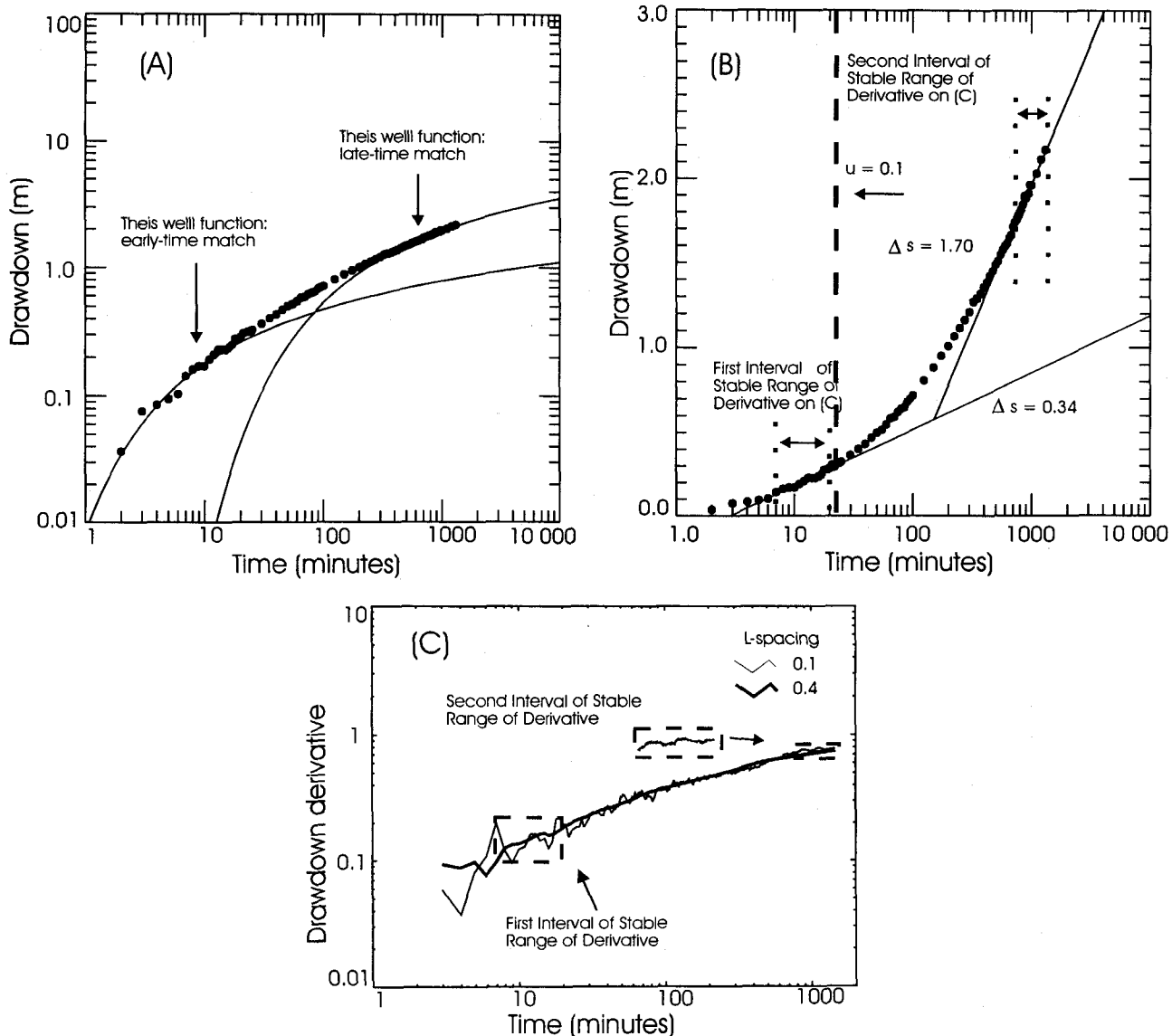
Fig. 8. Cooper-Jacob semilog plot of time–drawdown data (A) and log–log plot of drawdown derivative versus time (B) for the Carseland north well. Two semilog straight-line segments are interpreted in A that correspond to interpreted stable ranges of derivative values in B.



The derivative plot (Fig. 7B) removes some of the ambiguity. The time interval corresponding to the first semilog straight line in Fig. 7A has what may be a stable drawdown derivative for the first 5 min of pumping. The interval is so short, however, that there can be little confidence placed on this interpretation. For most of the test interval, the derivative profile shows a steep decline in the value of the derivative. This behaviour is indicative of leakage or the presence of a recharge boundary. Therefore, we conclude that the data of the second shorter segment on the Cooper-Jacob plot should not be used for estimation of aquifer hydraulic properties.

The transmissivity of the aquifer near the well, about 1.1 m²/d, has been estimated from the slope of the first semilog straight line, since we consider the late test data to

Fig. 9. Theis curve match (A), Cooper-Jacob semilog plot of time-drawdown data (B), and log-log plot of drawdown derivative versus time (C) for data from the Carseland north observation well. This curve is matched to early and late test data. Two semilog straight-line segments are identifiable on the Cooper-Jacob plot. However, only the early interval is associated with an interpreted stable range of derivative values in C. Calculation of the u criteria indicates the Cooper-Jacob solution is not valid for this first semilog straight-line segment.



be affected by leakage. The brief interval considered as possibly representative of IARF on the derivative profile is marked on the Cooper-Jacob plot in Fig. 7A for comparison. No estimate of storativity was made from these pumping-well data. There is insufficient geologic or hydrogeologic evidence to say whether the leakage observed in the West Well is coming from a lateral recharge boundary, perhaps a coarse-grained channel element in the aquifer, or from release from storage in overlying confining clay tills.

North well

The north well is located 1 km north of Carseland at DLS coordinates NE 12-22-26 W4M (see Fig. 2). The top of

the sand and gravel deposits are 67.7 m (222 feet) below ground and are at least 5 m thick. Traces of resistivity and gamma-ray logs through the aquifer zone are shown in Fig. 4C. The static water level was about 23 m above the base of the aquifer on the date of the test. The aquifer was stressed by pumping the well for 24 h at a constant rate of 576 m³/d (88 igpm). Water levels were monitored in the pumped well and in an observation well located 60 m north.

The Cooper-Jacob semilog plot for the north pumping well is shown in Fig. 8A. The corresponding derivative plot is shown in Fig. 8B. The Theis log-log, Cooper-Jacob plot and drawdown-derivative plots for the north observation

well are shown in Figs. 9A, 9B, and 9C. As with the south pumping well data, the north pumping well data are affected by noise associated with the pump in the well. Some of the noise in the data is also due to the release of exsolved methane during pumping. The presence of methane was confirmed by measuring combustible vapours at the well-head during pumping.

The Cooper-Jacob plot for the north pumping well has been interpreted as having two semilog straight-line segments with a lengthy transition zone. The derivative plot in Fig. 8B is difficult to interpret because of the noise. The profile may show an early time of stable derivative values from $t = 4$ min to about $t = 50$ min. A second interval of stable derivative may occur near the end of the test, starting at about $t = 800$ min, as marked in Fig. 8B. Using the interpretation of the derivative profile as our guide, two semilog straight lines have been marked in Fig. 8A. The first semilog straight line has a slope of 0.38 m/log cycle. The second has a slope of 1.90 m/log cycle. These slopes correspond to transmissivities of 277 and 55 m²/day, respectively.

The log-log time-drawdown plot for the north observation well has been fitted with the Theis curve for an early- and a late-time interval in Fig. 9A. The transmissivity corresponding to the early-time fit is also 277 m²/d, and the corresponding estimate of storativity is 4.5×10^{-4} . The transmissivity corresponding to the late-time interval is 65 m²/d. The Cooper-Jacob time-drawdown profile of the north observation well in Fig. 9B shows again an early and a late semilog straight-line segment with a lengthy transition zone. On the derivative profile in Fig. 9C we have interpreted two intervals of stable range of derivative. The first is from about $t = 7$ min to $t = 20$ min. The second is from about $t = 700$ min to the end of the test.

The first interval of stable range of the derivative value is used to define a time segment for Cooper-Jacob analysis in Fig. 9B. The slope of the corresponding semilog straight-line segment is 0.34 m/log cycle, and the calculated transmissivity is 310 m²/d. However, this interval of time lies in the range of $u > 0.1$. Therefore, this estimate of T from the Cooper-Jacob solution should not be accepted. This example underscores how easy it can be to overinterpret noisy derivative plots.

The second interval of stable range of the derivative is used to draw a semilog straight line through the late test data. The slope of this line is 1.70 m/log cycle, and the corresponding estimate of T is 62 m²/d. This estimate of T corresponds well with the estimate obtained from the Theis curve analysis of the same data.

In Fig. 8A the slope of the second semilog straight-line segment is more than twice the value of the first. The difference in the slopes suggests that the presence of a simple linear boundary, such as an aquifer pinch-out on the nearby north flank of the Calgary Valley (see Fig. 2), is insufficient to explain the observed time-drawdown behaviour.

Consideration of the geologic framework of the aquifer helps us interpret the hydraulic response. The first constant derivative interval represents a time of IARF to the north pumping well during pumping. The behaviour may represent drainage within the limits of a thick, coarse alluvial element penetrated by the well. After about 50 min of pumping (based on the north pumping well's derivative plot in

Table 1. Estimates of Q_{20} parameter.

Well	H^a (m)	T^b (m ² /d)	Q_{20}^c (m ³ /d)	T^d (m ² /d)	Q_{20}^e (m ³ /d)
South	19	56	726	32	415
West	22	1.1	17	—	—
North	15	227	2325	55	563

^aTotal available drawdown = static water level – elevation of top of screen or aquifer, whichever is least.

^bTransmissivity derived from first interval of IARF, where applicable.

^c Q_{20} calculated with T from first interval of IARF, where applicable.

^dTransmissivity derived from second interval of IARF, where applicable.

^e Q_{20} calculated with T from second interval of IARF, where applicable.

Fig. 8B), the first interval of IARF ends. At this time the cone of depression probably reaches the limit to the coarse materials surrounding the well. Thereafter, the derivative slowly rises to a new constant value as the cone of depression encompasses enough of the thinner and finer architectural elements (e.g., lateral accretion deposits, overbank fines) adjacent to the presumed coarse channel element at the well to again produce IARF.

Derivative-assisted estimation of well yields in heterogeneous aquifers

A simple way to make a baseline estimate of the long-term yield of a single well is to calculate (from the Cooper-Jacob equation) the continuous discharge, Q , that would use up all available drawdown in a specified length of time, assuming IARF. In Alberta, this heuristic parameter is usually calculated using 20 years (or about 8 log cycles of time expressed in days) as the specified length of time, and thus is called the Q_{20} :

$$[2] \quad Q_{20} = \frac{4\pi H/8}{2.30}$$

where Q is the continuous discharge rate [L^3/T], H is the available drawdown [L], and T is the aquifer transmissivity [L^2/T]. Operationally, this is equivalent to using the Cooper-Jacob expression to calculate transmissivity from a semilog time-drawdown plot, but in this operation Q is the unknown and the semilog time-drawdown curve has a fixed slope equal to $H/8$ per log₁₀ cycle.

The Q_{20} parameter was originally developed as a means to compare general aquifer quality in regional hydrogeologic mapping in the Province of Alberta in the 1960's (J. Toth, personal communication), but gained widespread use in groundwater permit applications in following decades. Once calculated, the Q_{20} is used as a basis for comparison of predicted yields assuming IARF with and without interference from neighbouring wells. Geologic heterogeneities and recharge boundaries are not explicitly considered. Well inefficiency may be accounted for by multiplying the available drawdown by a safety factor less than one before

calculating the Q_{20} , e.g., a safety factor of 0.70 allows 30% of available drawdown for well losses.

Our paper demonstrates how derivative analysis in aquifer testing can extend the application of a simple heuristic like the Q_{20} to heterogeneous systems in two ways. First, the drawdown derivative can be used to identify the type of hydraulic system encountered by a pumping well. This will help the hydrogeologist decide if a Q_{20} analysis is geologically appropriate. Second, the drawdown derivative helps identify true IARF in the aquifer-test data, allowing a more confident estimate of aquifer T and S .

In the case of the south well, two intervals of IARF were identified. The first interval is deemed to represent true IARF conditions in the aquifer. The second interval is deemed to be affected by a linear internal boundary. If we calculate the Q_{20} with $T = 56 \text{ m}^2/\text{d}$, the value derived from the first interval of IARF, we arrive at a value of $726 \text{ m}^3/\text{d}$. By applying image well theory in the presence of a simple linear boundary, we would find that a Q_{20} value of $363 \text{ m}^3/\text{d}$ would be appropriate. If we did not apply derivative or image-well analysis to this problem and calculated the Q_{20} using the value of T derived from the steepest slope observed on the Cooper-Jacob plot in Fig. 5A, $32 \text{ m}^2/\text{d}$, then we would arrive at a Q_{20} of $415 \text{ m}^3/\text{d}$ (Table 1). That this value is close in magnitude to the estimate of Q_{20} from image-well theory is not surprising, since the late-interval data with the steepest semilog slope incorporates the hydraulic effect of the linear boundary. The difference lies in our understanding of the hydraulics. With the former estimate, application of derivative analysis provides confidence in the estimate of T and S , and image well theory provides a basis for predicting long-term hydraulic response of the aquifer to pumping. The latter estimate, on the other hand, is ad hoc and indefensible should future problems arise with the groundwater permit.

In the case of the west well, the recognition that most of the test data were affected by recharge led to a realistic estimate of aquifer T and S . The T value of $1.1 \text{ m}^2/\text{d}$ from the early test data provided a Q_{20} estimate of only $17 \text{ m}^3/\text{d}$ (Table 1).

At the north well, analysis of the complex time-drawdown response was clarified by use of the derivative curve. With the derivative curve, an independent hydraulic argument could be made that the latest time-drawdown data provided the best estimate of aquifer bulk T and S , even though a very high value of T was observed which represented IARF very close to the pumping well. This argument is judged reasonable given the established geologic model of buried valley aquifers. The high, early-time value of T of $227 \text{ m}^2/\text{d}$ gives a Q_{20} of $2325 \text{ m}^3/\text{d}$. The lower, late-time value of T of $55 \text{ m}^2/\text{d}$ gives a Q_{20} of $563 \text{ m}^3/\text{d}$ (Table 1). It is of interest to note that the late-time value of T at the north well, $68 \text{ m}^2/\text{d}$, is close in magnitude to the value of T at the south well measured before the boundary was observed, $56 \text{ m}^2/\text{d}$. This similarity increases our confidence in using these values to assign long-term yields.

Conclusions

Estimation of long-term yields of wells based on single-well aquifer tests can be difficult. The cone of depression around

a pumping well expands over time, encountering boundaries and aquifer heterogeneities. This behaviour is expected in alluvial aquifer systems because of their internal complexity and relatively short characteristic lengths of hydraulic subdivisions. Deeper understanding of the probable long-term behaviour of water wells in such complex aquifers can be improved with drawdown-derivative techniques. The understanding is further improved when geological insight and maps are used as independent checks on the hydraulic interpretations.

Our examples clearly demonstrate that while uncritical acceptance of lowest transmissivity values derived from the steepest slopes of Cooper-Jacob plots can give provide reasonable predictions of long-term drawdown behaviour at pumping wells, this practice is indefensible as a part of standard hydrogeological analysis. Derivative analysis, properly applied, can guide the interpreter to better understanding of aquifer response to pumping. This understanding in turn will lead to application of the appropriate hydraulic model for predicting long-term hydraulic behaviour in any specific case. However, the practitioner should be cautioned against overinterpretation of the derivative plots. Drawdown-derivative analysis can be a very useful technique for conventional aquifer test analysis. It should become part of every hydrogeologist's "toolbox."

Acknowledgements

The authors thank CH2M HILL Engineering Ltd. of Calgary and the County of Wheatland, Alberta, for the data in this study. Support for Mr. Parks was provided by Amoco Canada Petroleum Company Ltd. and the Department of Geology and Geophysics at the University of Calgary. Other support was provided by the Natural Sciences Research Council of Canada operating grant OGP0122023. This paper benefited from the comments of two anonymous reviewers, and we thank them for their efforts.

References

- Anderson, M.P. 1990. Aquifer heterogeneity—a geological perspective. Proceedings, 5th Canadian-American Conference on Hydrogeology, Banff, Alta., September, pp. 3–22.
- Bourdet, D., Whittle, T.M., Douglas, A.A., and Picard, Y. 1983. A new set of type-curves simplifies well test analysis. *World Oil*, May: 95–106.
- Bourdet, D.J., Ayoub, A., and Picard, Y.M. 1989. Use of pressure derivative in well-test interpretation. *Society of Petroleum Engineers Formation Evaluation*, June, pp. 293–302.
- Carlson, V.A., Turner, W.R., and Geiger, K.W. 1969. A gravel and sand aquifer in the Bassano-Gem Region, Alberta. Alberta Research Council, Edmonton, Report 69-4.
- deMarsily, G. 1986. *Quantitative hydrogeology*. Academic Press, Toronto.
- Desbarats, A.J. 1994. Spatial averaging of hydraulic conductivity under radial flow conditions. *Mathematical Geology*, 26: 1–21.
- Ehlig-Economides, C. 1988. Use of pressure derivative for diagnosing pressure-transient behaviour. *Journal of Petroleum Technology*, October: 1280–1282.
- Geiger, K.W. 1968. Bedrock topography of the Gleichen map-area, Alberta. Alberta Research Council of Alberta, Edmonton, Report 67-2.

- Karasaki, K., Long, J.C.S., and Witherspoon, P.A. 1988. Analytical models of slug tests. *Water Resources Research*, **24**: 115-126.
- Kucuk, F.J., and Kabir, S. 1988. Well test interpretation for reservoir with a single linear no-flow barrier. *Journal of Petroleum Science and Engineering*, pp. 195-221.
- Kruseman, G.P., and de Ridder, N.A. 1990. Analysis and evaluation of pumping test data. 2nd ed. International Institute for Land Reclamation and Improvement, Wageningen, The Netherlands.
- Lennox, D.H., Maathuis, H., and Pederson, D. 1988. Region 13, Western Glaciated Plains. *In Hydrogeology. Edited by W. Back, J.S. Rosenhein, and P.R. Seaber. Geological Society of America, Boulder, Colo., The Geology of North America, Vol. O-2.*
- Ostrowski, L.P., and Kloska, M.B. 1989. Use of pressure derivatives in analysis of slug test or DST flow period data. Society of Petroleum Engineers, Paper 18595.
- Ozoray, G.F., and Lytviak, A.T. 1974. Hydrogeology of the Gleichen Area, Alberta. Alberta Research Council, Edmonton, Report 74-9.
- Shaver, R.B., and Puse, S.W. 1992. Hydraulic barriers in Pleistocene buried valley aquifers. *Ground Water*, **30**: 21-28.
- Spane, F.A., Jr., and Wurstner, S.K. 1993. DERIV: A computer program for calculating pressure derivatives for use in hydraulic test analysis. *Ground Water*, **31**: 814-822.
- Wong, D.W., Harrington, A.G., and Cinco-Ley, H. 1986. Application of the pressure-derivative function in the pressure-transient testing of fractured wells. Society of Petroleum Engineers Formation Evaluation, October, pp. 470-480.